

## **Amygdala intercalated neurons are required for expression of fear extinction**

Rutgers University has made this article freely available. Please share how this access benefits you.  
Your story matters. [\[https://rucore.libraries.rutgers.edu/rutgers-lib/29483/story/\]](https://rucore.libraries.rutgers.edu/rutgers-lib/29483/story/)

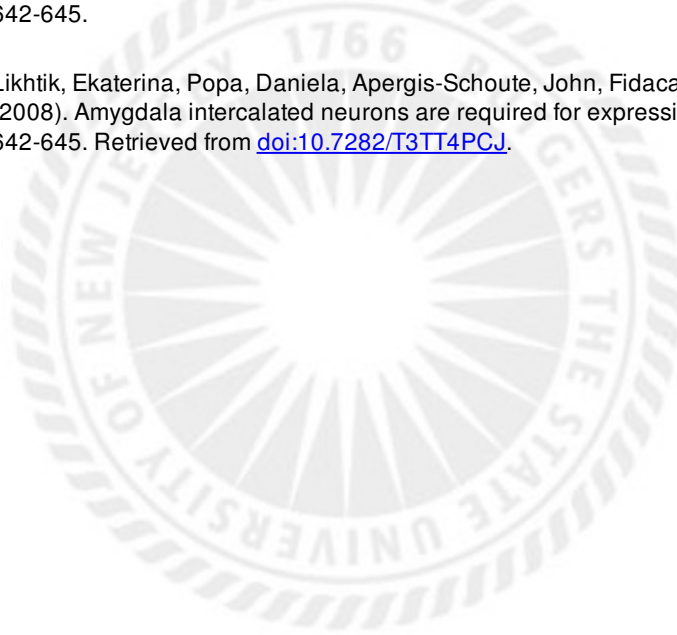
This work is an **ACCEPTED MANUSCRIPT (AM)**

This is the author's manuscript for a work that has been accepted for publication. Changes resulting from the publishing process, such as copyediting, final layout, and pagination, may not be reflected in this document. The publisher takes permanent responsibility for the work. Content and layout follow publisher's submission requirements.

Citation for this version and the definitive version are shown below.

**Citation to Publisher** Likhtik, Ekaterina, Popa, Daniela, Apergis-Schoute, John, Fidacaro, George A. & Paré, Denis.  
**Version:** (2008). Amygdala intercalated neurons are required for expression of fear extinction. *Nature* 454, 642-645.

**Citation to *this* Version:** Likhtik, Ekaterina, Popa, Daniela, Apergis-Schoute, John, Fidacaro, George A. & Paré, Denis.  
(2008). Amygdala intercalated neurons are required for expression of fear extinction. *Nature* 454, 642-645. Retrieved from [doi:10.7282/T3TT4PCJ](https://doi.org/10.7282/T3TT4PCJ).



**Terms of Use:** Copyright for scholarly resources published in RUcore is retained by the copyright holder. By virtue of its appearance in this open access medium, you are free to use this resource, with proper attribution, in educational and other non-commercial settings. Other uses, such as reproduction or republication, may require the permission of the copyright holder.

*Article begins on next page*

**AMYGDALA INTERCALATED NEURONS ARE  
REQUIRED FOR EXPRESSION OF FEAR EXTINCTION**

**Ekaterina Likhtik, Daniela Popa, John Apergis-Schoute, George A Fidacaro Jr, Denis Paré**

Center for Molecular and Behavioral Neuroscience, Rutgers,  
The State University of New Jersey, Newark, New Jersey 07102.

Correspondence should be sent to:

Denis Paré  
CMBN, Aidekman Research Center  
Rutgers, The State University of New Jersey  
197 University Avenue  
Newark, NJ 07102

Phone: 973-353-1080 x3251  
Fax: (973) 353-1255  
Email: [pare@axon.rutgers.edu](mailto:pare@axon.rutgers.edu)

Congruent findings from studies of fear learning in animals and humans indicate that research on the circuits mediating fear constitutes our best hope of understanding human anxiety disorders<sup>1-4</sup>. In mammals, repeated presentations of a conditioned stimulus (CS) that was previously paired to a noxious stimulus leads to the gradual disappearance of conditioned fear responses. Although much evidence suggests that this extinction process depends on plastic events in the amygdala<sup>1-7</sup>, the underlying mechanisms remain unclear. Intercalated (ITC) amygdala neurons constitute likely mediators of extinction because they receive CS information from the basolateral amygdala (BLA)<sup>8,9</sup>, and contribute inhibitory projections to the central nucleus (CEA)<sup>10,11</sup>, the main output station of the amygdala for conditioned fear responses<sup>12</sup>. Thus, following extinction training, ITC cells could reduce the impact of CS-related BLA inputs to CEA via feed-forward inhibition. Here, we tested the hypothesis that ITC neurons mediate extinction by lesioning them with a toxin that selectively targets cells expressing  $\mu$ -opioid receptors ( $\mu$ ORs). Electron microscopic observations revealed that the incidence of  $\mu$ OR-immunoreactive synapses is much higher in ITC cell clusters than in BLA or CEA and that  $\mu$ ORs typically have a post-synaptic location in ITC cells. In keeping with this, bilateral infusions of the  $\mu$ OR agonist dermorphin conjugated to the toxin saporin in the vicinity of ITC neurons caused a 34% reduction in the number of ITC cells but no significant cell loss in surrounding nuclei. Moreover, ITC lesions caused a marked deficit in the expression of extinction that correlated negatively with the number of surviving ITC neurons but not CEA cells. Because ITC cells exhibit an unusual pattern of receptor expression, these findings open new avenues for the treatment of anxiety disorders.

The hypothesis that ITC cells are involved in extinction<sup>13</sup> has not been tested yet because ITC cells occur as small, distributed cell clusters, making selective electrolytic or excitotoxic ITC lesions impossible. Here, we circumvent this difficulty by exploiting the fact that ITC neurons express high levels of  $\mu$ ORs (**Fig. 1a**)<sup>14, 15</sup> allowing selective ITC lesions with a peptide-toxin conjugate that only targets  $\mu$ OR-expressing cells. Indeed, targeted toxins take advantage of receptor-mediated endocytosis to deliver cytotoxins to specific types of neurons<sup>16</sup>. Here, the peptide dermorphin, an agonist with a high affinity and selectivity for  $\mu$ ORs<sup>17</sup>, was conjugated to the ribosome inactivating protein saporin (D-Sap).

For this lesion method to be effective,  $\mu$ ORs must be located postsynaptically in ITC cells, not in their afferents. Thus, we first used electron microscopy to determine their subcellular location. In the electron microscope,  $\mu$ OR-immunoreactivity was more concentrated in ITC cell clusters than BLA or CEA (see **Fig. S1**) and it was generally found postsynaptically (**Figs. 1b,c; Fig. S2**). Indeed, the proportion of synapses that displayed postsynaptic  $\mu$ OR immunolabeling was  $\approx$ 3-6 times higher in the ITC cell clusters than in CEA ( $p=0.009$ ) or BLA ( $p=0.0001$ ;  $X^2$ -tests; **Fig. 1c**).

Having established that postsynaptic  $\mu$ OR expression is much higher in the ITC cell clusters than neighboring nuclei, we tested the feasibility of obtaining selective ITC lesions with the targeted toxin D-Sap and examined their impact on extinction. Briefly, 58 rats were habituated to the training chamber (Day-1) and fear conditioned to a tone (Day-2). Then, in a different context, they were trained on extinction (Day-3). On Day-4, they received bilateral infusions of either D-Sap (Experimental group) or the same volume and concentration of a scrambled peptide conjugated to saporin (U-Sap, Control group) aimed at ITC cells. On Day-11, extinction recall was tested. The conditioned response we monitored was behavioral freezing,

quantified by an observer blind to the rats' condition.

To maximize lesion specificity, we only considered rats in which the cannula tips were at the BLA-CEA border (i.e. where CEA-inhibiting ITC cells are located), without knowledge of the behavioral data. In the control U-Sap and experimental D-Sap groups, respectively 11 and 8 rats met this criterion. **Figure 2** shows coronal sections obtained from such control (**Fig. 2a-c**) and experimental (**Fig. 2d-f**) rats. Compared to control (U-Sap) cases, D-Sap infusions caused a marked but spatially circumscribed reduction in  $\mu$ OR staining restricted to the region adjacent to the infusion site (white arrows), where peri-CEA ITC clusters are normally found (black arrows). More distant ITC clusters such as those bordering the external capsule (arrowheads) or at the posterior pole of the amygdala (**Fig. 2c,f**) were not affected. Importantly, no difference in  $\mu$ OR labeling was seen in CEA or BLA between experimental and control rats. Nevertheless, to control for possible effects of cell loss due to unintended D-Sap diffusion, we also analyzed the behavior of rats where histological controls revealed that D-Sap infusions missed the BLA-CEA border but instead ended in CEA (n=8; **Fig. 2h**) or BLA (n=7; **Fig. 2i**).

To evaluate the neuronal loss caused by D-Sap infusions in ITC clusters, we performed unbiased stereological estimates of ITC and CEA neuronal numbers on sections counterstained with cresyl violet. The observer was blind to the rats' condition. Compared to U-Sap-treated rats, a significant reduction in the number of ITC cells was found in rats that received D-Sap infusions in ITC clusters (**Fig. 2g**; U-Sap,  $18,499 \pm 1,406$ , n=8; D-Sap,  $12,197 \pm 1,523$ , n=6; -34%, t-test, p=0.01). In contrast, neuronal counts in CEA were nearly identical in the two groups (U-Sap,  $37,949 \pm 3,516$ , n=4; D-Sap,  $40,471 \pm 2,328$ , n=5; t-test, p=0.55).

**Fig. 3a** shows percent time freezing (y-axis) during the different experimental phases in the three groups: the experimental group that received D-Sap infusions in the medial ITC clusters

(red, n=8) and the two control groups that received either U-Sap infusions at the same site (empty black circles, n=11) or D-Sap infusions centered on BLA or CEA (filled black circles, n=15). Prior to D-Sap or U-Sap infusions, the three groups behaved similarly during habituation, fear conditioning, and extinction training (**Fig. 3a, Days 1-3**). However, after ITC lesions (Day-4), their behavior differed significantly during recall of extinction (**Fig. 3a, Day-11**) with ITC-lesioned rats showing impaired expression of extinction (two-way repeated measures ANOVA,  $F_{(2,270)}=11.399$ ,  $p=0.0002$ ). Post-hoc t-tests with stepwise Bonferroni correction of the significance level ( $p<0.05$ ) comparing the D-Sap ITC group vs. the average of the two control groups in blocks of two trials revealed that rats with ITC lesions had significantly higher freezing levels during the first four CSs. Moreover, a strong inverse correlation was found between freezing levels during extinction testing and the number of surviving ITC cells (**Fig. 3b, filled circles**,  $r=-0.67$ ,  $p<0.01$ ,  $n=14$ ). In contrast, no such relationship was seen with CEA cell counts (**Fig. 3b, empty circles**;  $r=-0.13$ ,  $p>0.05$ ,  $n=9$ ).

Inter-group differences were not attributable to non-specific increases in anxiety levels secondary to ITC lesions as exploratory behavior in a novel open field was indistinguishable between the three groups (ANOVAs,  $F_{(2,25)}$ : % time in center  $F=1.28$ ,  $p=0.29$ , distance traveled  $F=1.11$ ,  $p=0.34$ ). Moreover, the three groups acquired conditioned fear responses to a different CS at the same rate (**Fig. 3, Day-13**; ANOVA,  $F_{(2,93)}=0.007$ ,  $p=0.9931$ ). Finally, the extinction deficit seen in the experimental group did not result from a non-specific CEA disinhibition since freezing during the last CS of the first (Day-2) and second (Day-13) fear conditioning sessions was identical (paired t-test,  $p=0.61$ ).

While ITC lesions produced a deficit in extinction expression, the difference between the three groups progressively decreased with repeated CS presentations. Several factors probably

contributed to the development of extinction after ITC lesions. First, much evidence indicates that the gradual fear reduction seen within an extinction training session depends on different mechanisms than those underlying between-session extinction. Indeed, some lesions<sup>3</sup> and pharmacological treatments<sup>6</sup> leave within-session extinction intact or marginally reduced, yet severely reduce between-session extinction. This implies that extinction engages at least two parallel processes. A first process that develops rapidly but is short lasting, responsible for within-session extinction, and a second process that lasts longer and underlies between-session extinction. Although the mechanisms underlying within-session extinction remain unclear, a likely contributing factor is the progressive reduction in BLA unit responses as the CS is repeated. In addition, a participation of ITC cells to within-session extinction cannot be ruled out. Indeed, because our ITC lesions were incomplete, surviving ITC neurons might have contributed to within-session extinction. However, since the deficit caused by ITC cells was most pronounced at the onset of the testing session, ITC cells are probably critical to between-session extinction, as described below.

Extinction is known to depend on the reinforcement of an active GABAergic process<sup>18</sup> and on NMDA-dependent synaptic plasticity in the amygdala<sup>5-7, 19</sup>. However, extinction training does not erase the initial fear memory because many BLA neurons maintain their increased CS responsiveness after extinction training<sup>20, 21</sup>. Importantly, extinction training does not interfere with conditioned fear responses (CRs) to a different CS or with the subsequent acquisition of CRs to a different CS<sup>1</sup>.

We propose that ITC neurons can account for these properties of extinction. Indeed, ITC neurons receive CS information from BLA<sup>8, 9</sup> and send GABAergic projections to CEA<sup>10, 11</sup>. Thus, they are in a perfect position to regulate the flow of CS information from the BLA to

CEA<sup>9</sup>. Importantly, ITC neurons receive a dense projection from the infralimbic (IL) cortex<sup>22</sup>, whose stimulation accelerates extinction<sup>23</sup> and inhibits CEA neurons<sup>24</sup>. We hypothesize that the CS-specificity of extinction derives from the ability of BLA synapses onto ITC neurons to express activity- and NMDA-dependent LTP<sup>13, 25</sup>. During extinction training, convergence of CS-related IL and BLA inputs onto ITC cells would facilitate induction of NMDA-dependent LTP, but only at those BLA to ITC synapses recruited by the CS. This CS-specific potentiation of BLA inputs onto ITC cells would enhance the depolarization produced by the CS in ITC cells. Consequently, the GABAergic output of ITC cells onto CEA neurons would be increased, ultimately leading to a CS-specific reduction of conditioned fear responses. In light of recent findings showing increased bursting and tone responsiveness of IL neurons after extinction training<sup>23, 26</sup>, it is possible that IL facilitates extinction-related plasticity, during a consolidation phase.

Although the details of this model remain to be tested, the finding that ITC lesions produce a deficit in the expression of extinction that correlates negatively with the number of surviving ITC cells suggests that ITC cells are critically involved in extinction. The significance of this conclusion derives from earlier results suggesting that some human anxiety disorders reflect an extinction deficit<sup>3, 4, 27</sup> and functional imaging evidence that the medial prefrontal cortex and amygdala are respectively hypo- and hyper-active in such disorders<sup>28, 29</sup>. As a result, it might be possible to compensate for these abnormalities and facilitate extinction with pharmacological interventions that enhance the excitability of ITC cells by taking advantage of their unusual pattern of receptor expression<sup>14, 15, 30</sup>.



## **METHODS SUMMARY**

Procedures were approved by the Institutional Animal Care and Use Committee of Rutgers University, in compliance with the Guide for the Care and Use of Laboratory Animals (DHHS). For light (LM) and electron microscopic (EM) observations of  $\mu$ OR distribution, Sprague-Dawley rats were anesthetized, perfused-fixed, their brains sectioned, and the sections processed as described in the supplementary material. Some sections were counterstained with cresyl violet and used for estimation of neuron numbers with the optical fractionator method. For EM observations, regions of interest were observed in four blocks obtained from two animals. For the behavioral study, 58 rats were subjected to a fear conditioning paradigm as described in the supplementary material. One day after extinction training, the rats were anesthetized, mounted in a stereotaxic apparatus, their skull exposed, a craniotomy performed, and drugs infused in the ITC region with a micro-syringe. Data are expressed as mean  $\pm$  SEM.

### **Acknowledgements**

This work was supported by RO1 grant MH-073610 to D Paré and NRSA fellowship F31 MH76415 to EL from NIMH.

### **Competing interests statement**

The authors declare that they have no competing financial interests.

Correspondence and request for materials should be addressed to Denis Paré (e-mail: [pare@axon.rutgers.edu](mailto:pare@axon.rutgers.edu)).

## REFERENCES

1. Myers, K. M. & Davis, M. Mechanisms of fear extinction. *Mol Psychiatry* 12, 120-50 (2007).
2. Phelps, E. A. & LeDoux, J. E. Contributions of the amygdala to emotion processing: from animal models to human behavior. *Neuron* 48, 175-87 (2005).
3. Quirk, G. J. & Mueller, D. Neural mechanisms of extinction learning and retrieval. *Neuropsychopharmacology* 33, 56-72 (2008).
4. Ressler, K. J. & Mayberg, H. S. Targeting abnormal neural circuits in mood and anxiety disorders: from the laboratory to the clinic. *Nat Neurosci* 10, 1116-24 (2007).
5. Falls, W. A., Miserendino, M. J. D. & Davis, M. Extinction of fear-potentiated startle: blockade by infusion of an NMDA antagonist into the amygdala. *J Neurosci* 12, 854-863 (1992).
6. Sotres-Bayon, F., Bush, D. E. & LeDoux, J. E. Acquisition of fear extinction requires activation of NR2B-containing NMDA receptors in the lateral amygdala. *Neuropsychopharmacology* 32, 1929-40 (2007).
7. Walker, D. L., Ressler, K. J., Lu, K. T. & Davis, M. Facilitation of conditioned fear extinction by systemic administration or intra-amygdala infusions of D-Cycloserine as assessed with fear-potentiated startle in rats. *J Neurosci* 22, 2343-2351 (2002).
8. Marowsky, A., Yanagawa, Y., Obata, K. & Vogt, K. E. A specialized subclass of interneurons mediates dopaminergic facilitation of amygdala function. *Neuron* 48, 1025-1037 (2005).
9. Royer, S., Martina, M. & Paré, D. An inhibitory interface gates impulse traffic between the input and output stations of the amygdala. *J Neurosci* 19, 10575-10583 (1999).
10. Paré, D. & Smith, Y. Distribution of GABA immunoreactivity in the amygdaloid complex of the cat. *Neuroscience* 57, 1061-1076 (1993).
11. Paré, D. & Smith, Y. The intercalated cell masses project to the central and medial nuclei of the amygdala in cats. *Neuroscience* 57, 1077-1090 (1993).
12. Davis, M. in *The Amygdala: a functional analysis* (ed. Aggleton, J. P.) 213-287 (Oxford University Press, Oxford, 2000).
13. Royer, S. & Pare, D. Bidirectional synaptic plasticity in intercalated amygdala neurons and the extinction of conditioned fear responses. *Neuroscience* 115, 455-462 (2002).
14. Jacobsen, K. X., Hoistad, M., Staines, W. A. & Fuxe, K. The distribution of dopamine D1 receptor and mu-opioid receptor 1 receptor immunoreactivities in the amygdala and interstitial nucleus of the posterior limb of the anterior commissure: relationships to tyrosine hydroxylase and opioid peptide terminal systems. *Neuroscience* 141, 2007-2018 (2006).
15. Poulin, J. F., Chevalier, B., Laforest, S. & Drolet, G. Enkephalinergic afferents of the centromedial amygdala in the rat. *J Comp Neurol* 496, 859-876 (2006).
16. Wiley, R. G. & Lappi, D. A. Targeted toxins in pain. *Adv Drug Deliv Rev* 55, 1043-1054 (2003).
17. Gaudriault, G., Nouel, D., Dal Farra, C., Beaudet, A. & Vincent, J. P. Receptor-induced internalization of selective peptidic mu and delta opioid ligands. *J Biol Chem* 272, 2880-2888 (1997).
18. Harris, J. A. & Westbrook, R. F. Evidence that GABA transmission mediates context-specific extinction of learned fear. *Psychopharmacology (Berl.)* 140, 105-115 (1998).

19. Lee, H. & Kim, J. J. Amygdalar NMDA receptors are critical for new fear learning in previously fear-conditioned rats. *J Neurosci* 18, 8444-8454 (1998).
20. Hobin, J. A., Goosens, K. A. & Maren, S. Context-dependent neuronal activity in the lateral amygdala represents fear memories after extinction. *J Neurosci* 23, 8410-8416 (2003).
21. Repa, J. C. et al. Two different lateral amygdala cell populations contribute to the initiation and storage of memory. *Nat Neurosci* 4, 724-731 (2001).
22. McDonald, A. J., Mascagni, F. & Guo, L. Projections of the medial and lateral prefrontal cortices to the amygdala: A Phaseolus vulgaris leucoagglutinin study in the rat. *Neuroscience* 71, 55-75 (1996).
23. Milad, M. R. & Quirk, G. J. Neurons in medial prefrontal cortex signal memory for fear extinction. *Nature* 420, 70-74 (2002).
24. Quirk, G. J., Likhtik, E., Pelletier, J. G. & Pare, D. Stimulation of medial prefrontal cortex decreases the responsiveness of central amygdala output neurons. *J Neurosci* 23, 8800-8807 (2003).
25. Royer, S. & Pare, D. Conservation of total synaptic weights via inverse homo- vs. heterosynaptic LTD and LTP. *Nature* 422, 518-522 (2003).
26. Burgos-Robles, A., Vidal-Gonzalez, I., Santini, E. & Quirk, G. J. Consolidation of fear extinction requires NMDA receptor-dependent bursting in the ventromedial prefrontal cortex. *Neuron* 53, 871-80 (2007).
27. Milad, M. R. et al. Presence and acquired origin of reduced recall for fear extinction in PTSD: Results of a twin study. *J Psychiatr Res* 42, 515-20 (2008).
28. Bremner, J. D., Elzinga, B., Schmahl, C. & Vermetten, E. Structural and functional plasticity of the human brain in posttraumatic stress disorder. *Prog Brain Res* 167, 171-86 (2008).
29. Shin, L. M., Rauch, S. L. & Pitman, R. K. Amygdala, medial prefrontal cortex, and hippocampal function in PTSD. *Ann N Y Acad Sci* 1071, 67-79 (2006).
30. Fuxe, K. et al. The dopamine D1 receptor-rich main and paracapsular intercalated nerve cell groups of the rat amygdala: relationship to the dopamine innervation. *Neuroscience* 119, 733-46 (2003).

## FIGURE LEGENDS

**Fig. 1**  $\mu$ OR immunoreactivity in the amygdala. **(a)** Coronal section processed to reveal  $\mu$ OR immunoreactivity (brown) and counterstained with cresyl violet (blue).  $\mu$ OR immunoreactivity is much higher in ITC cell clusters than surrounding nuclei. **(b)** Electron micrograph showing examples of  $\mu$ OR<sup>+</sup> synapses in the ITC region. **(c)** Proportion of synapses (mean  $\pm$  s.e.m.) where  $\mu$ OR immunoreactivity was found in the post- (gray) or presynaptic element (black) in the ITC, BLA, or CEA.

**Fig. 2** D-Sap infusions at BLA-CEA border cause a spatially circumscribed loss of  $\mu$ OR immunoreactivity. **(a-f)** Coronal sections obtained from rats that received either U-Sap (Control, **a-c**) or D-Sap (Experimental, **d-f**) infusions at BLA-CEA border. Two left-most sections obtained near the infusion site (white arrow); right section, near the caudal pole of the amygdala. Arrowheads and black arrows point to lateral and medial ITC clusters, respectively. Dashed lines indicate trajectory of infusion cannulas. **(g)** Unbiased stereological estimates of cell numbers (mean  $\pm$  s.e.m.) in the medial ITC clusters and CEA in control (black) vs. experimental (red) animals. **(h-i)** D-sap infusion sites (white arrows) in the CEA **(h)** and BLA **(i)**.

**Fig. 3** D-Sap induced ITC lesions cause an extinction deficit. **(a)** Percent time freezing (y-axis; mean  $\pm$  s.e.m.) in ITC-lesioned rats (red; n=8) vs. control rats that received U-Sap infusions at the same site (empty black circles; n=11) or D-Sap infusions in the BLA or CEA (n=15; filled black circles). Data obtained in the D-Sap BLA and CEA animals was pooled because the behavior of these two rat subsets was statistically undistinguishable (ANOVA  $F_{(1,108)}=0.847$ ,

p=0.38). **(b)** Relationship between number of ITC (bottom) or CEA (top) neurons (y-axis) vs. percent time freezing (x-axis) during extinction testing session (average of first three trials).

## METHODS

*Histology.* To reveal  $\mu$ OR immunoreactivity, Sprague-Dawley rats were given an overdose of pentobarbital (100 mg/kg, i.p.) and perfused through the heart with 250 ml of 0.9% saline (4°C), followed by 500 ml of paraformaldehyde (4%) and picric acid (0.2%) in PBS (0.1 M, pH 7.4, 4°C). The brain was then extracted from the skull and a block containing the amygdala was prepared. The block was then glued to the stage of a vibrating microtome with a cyanoacrylate adhesive and cut in 60  $\mu$ m sections with a vibrating microtome. The sections were stored in PBS and then incubated in 1% sodium borohydride (in PBS) for 30 min, washed in PBS, pre-incubated in a blocking solution (10% goat serum, 1% BSA, Triton-X100, 0.3% for light microscopy, 0.04% for electron microscopy), and incubated overnight in the primary antibody solution containing  $\mu$ OR antibody from ImmunoStar (Hudson, WI; 1:4000), 1% normal goat serum, 1% BSA, and Triton-X100 (0.3% and 0.04% for light vs. electron microscopy) in PBS. Then, sections were incubated in the secondary antibody solution (Jackson, West Grove, PA, 1:200), followed by the avidin-biotin-complex (Vector, Burlingame, CA). The immunoreactivity was then revealed with diaminobenzidine (Sigma, St. Louis, MO) in tris [hydroxymethyl]-aminomethane (pH 7.6) buffer. A one-in-four series of sections was then counterstained with cresyl violet. Sections for electron microscopy were rinsed in PB, post-fixed in 2% osmium tetroxide for one hour, rinsed in PB, dehydrated in a graded series of alcohol and propylene oxide, embedded in resin, and baked for 48 hours at 60°C. Blocks containing the regions of interest were sectioned at 60-70 nm using an ultramicrotome, collected onto copper mesh grids, and counterstained with 5% uranyl acetate and Reynold's lead citrate.  $\mu$ OR+ structures were easy to differentiate from unlabeled elements because of the electron-dense amorphous diaminobenzidine reaction product associated with them (**Figs. 1b, S1-S3**).

*Fear conditioning and open field test.* We used Coulbourn (Allentown, PA) conditioning chambers (25 x 29 x 28 cm, with aluminum and Plexiglas walls) whose appearance was modified by introducing salient sensory clues (see below). The conditioning chambers were placed in sound attenuating boxes that contained a ventilation fan, and was illuminated by a single house light. On Day 1, rats were habituated to the training chamber (Context-A) for 20 minutes. On day 2, they were presented with 4 tone CS (4 kHz, 30 s), each co-terminating with a footshock (US, 0.4 mA, 1 s). On day 3, rats were placed in a different conditioning box (Context-B) and presented with 20 CS (with no US). On Day 11, their recall of extinction was probed with 10 presentations of the CS alone in Context B. On Day 13, the rats were fear conditioned to a different tone (1 kHz) in a different training context (Context-C). After testing in a novel open field, rats were perfused-fixed as described above for subsequent histology. Rats were subjected to this protocol in pairs, one from each group. The conditioned response we monitored was behavioral freezing, quantified off-line with a stopwatch by an observer blind to the rats' identity. For fear conditioning (Context-A), we used the chamber described above. For extinction training (Context-B), we introduced a black plexiglass floor washed with peppermint soap in the chamber. For the second fear conditioning (Context-C), the chamber had striped plexiglass walls. For the open field test, the rats were placed one by one in a novel large plexiglass enclosure (120x120 cm) with walls all around (35 cm high). Their spontaneous exploratory behavior was monitored with a video camera for 5 minutes. Attention was paid to the amount of time the rats spent along the walls versus the center of the open field as well as to the traveled distance and speed of travel.

*ITC lesions.* In order to be included in the lesion study, rats had to display  $\leq$  15% freezing

at the end of the extinction training session. A total of 58 rats met this criterion. On Day 4, rats were anesthetized with isoflurane and administered atropine methyl nitrate to reduce secretions and aid breathing. The rats were then mounted in a stereotaxic apparatus. Betadine was applied to the scalp and a local anesthetic (bupivacaine, s.c.) was injected to the region to be incised. Ten minutes later, the skull was exposed, a craniotomy performed, and a micro-syringe (25-gauge) stereotaxically directed to ITC clusters. Then, rats received bilateral infusions (0.01  $\mu$ l/min; total of 0.25  $\mu$ l/hemisphere) of either D-Sap (Experimental; 3 pmol/ $\mu$ l in sterile saline) or the same volume and concentration of a scrambled peptide conjugated to saporin (U-Sap, Control; Advanced Targeting systems, San Diego, CA). Ten minutes elapsed between the end of the infusion and removal of the micro-syringe to minimize diffusion along the needle tract. The wound was then sutured and a local antibiotic applied.

*Cell counts.* In a 1-in-4 series of sections stained to reveal  $\mu$ OR immunoreactivity and counterstained with cresyl violet, the regions of interest were outlined using a microscope equipped with a motorized stage and StereoInvestigator software (MicroBrightField, Williston, VT). Contour areas were measured with StereoInvestigator software, summed, and multiplied by the section thickness (60  $\mu$ m) and by the section sampling factor (4) to yield volume estimates. The optical fractionator method was used to estimate neuron numbers. Briefly, neurons were counted in a 1-in-4 series of sections starting from a random position near the rostral pole of the amygdala. We counted neurons throughout the sections except for guard zones at the upper and lower surfaces (3  $\mu$ m). The optical dissector height was 10.7  $\mu$ m. To estimate the number of stained amygdala neurons, the regions of interest were sampled randomly and systematically (ITC counting frame, 25 by 25  $\mu$ m; grid size, 45 by 43  $\mu$ m; CE, counting frame, 35 by 35  $\mu$ m; grid size, 115 by 115  $\mu$ m). Section thickness was re-measured each counting frame. For ITC counts, the Gundersen coefficients of error were  $0.5 \pm 0.01$  and  $0.04 \pm 0.01$  for the D-Sap and U-Sap groups, respectively. For the CEA counts, they were  $0.04 \pm 0.01$  for both groups.